HOMOGENIZATION OF STREAMLINES FIELD IN A CYLINDRICAL VESSEL WITH AXIAL HIGH-SPEED IMPELLER* **

I. FOŘT[a], O. JAROCH[b] and M. HOŠŤÁLEK[a]

[a] *Department of Chemical Engineering and*
[b] *Department of Mathematics,*
Prague Institute of Chemical Technology, 166 28 Prague 6

Received February 17th, 1976

The convection flow patterns are described in the space above a rotating axial high-speed impeller in a cylindrical vessel provided with radial baffles at its walls or with a draft-tube above the impeller. In both investigated systems liquid is forced by the impeller blades to the bottom of the vessel. The convection flow is described by means of a time-averaged streamlines distribution obtained as an analytical solution of a partial differential equation with corresponding boundary conditions. The resulting streamlines distribution indicates that the draft-tube used causes a significant improvement of the spacial homogeneity of flow in the agitated system, namely close to the liquid surface. In case of turbulent flow, the shape of streamlines in the investigated space is not exceedingly affected by the relative impeller-to-vessel size.

The convective or circulation flow in a technological equipment with axial high-speed agitator often influences both the efficiency of the apparatus and the quality of the product, *e.g.* crystals or products of a chemical reaction. The shape of the vessel, of its interior parts and of the impeller as well, should secure intensive circulation of the charge. In particular, an appropriate draft-tube may influence the originally inhomogeneous distribution of streamlines in such a way that the flow produced by the rotation of the impeller blades would run through every part of the vessel.

The convective flow of the liquid agitated by an axial high-speed impeller (Fig. 1) was investigated both qualitatively[1,2] and quantitatively[3-8], either in the entire volume of the vessel or in some of its important parts, *e.g.* at the bottom, near the walls, close to the liquid surface *etc.* For the circulation under turbulent conditions in a cylindrical vessel with radial baffes at its walls, and for the direction of flow from the impeller to the bottom, these results can be summarized as follows: *1.* In the convection flow, with the exception of the space occupied by the impeller itself and that immediately linking up (between the rotor and the bottom) axial and radial velocity components predominate. *2.* Mechanical energy dissipation in unit volume of the space under the rotating impeller is over 25times higher than in the space above it; this ratio increases with decreasing impeller-to-vessel diameter ratio. *3.* In the space under the rotation impeller the flow of the stirred charge shows a significant velocity gradient caused among others by a steep

* Part XLVI in the series Studies on Mixing; Part XLV: This Journal *42*, 2474 (1977).

** Presented at the Conference on Mixing and Polymer Processing, Delft 1976.

and non-monotonous velocity profile in the currents travelling through this space. *4.* The velocity gradient in the space above the rotating impeller is insignificant. This is illustrated by a very flat (nearly piston-like) velocity profile in the downward flow immediately above the stirrer. *5.* Except for the immediately adjacent region, the influence of the baffles on the axial symmetry of the convection flow may be neglected, as long as the axis of the agitator coincides with that of the vessel. Considering these facts a draft-tube has been designed for a model-size crystallizer with a high speed axial stirrer[8,9] consisting of a cylindrical part surrounding the impeller and a conical part above it (Fig. 2). The vessel has a conical bottom fitted in its lower part with a discharge opening $D_2 = D/6$, with vertex[10] angle $\beta = 120°$. From the measurements of the liquid circulation by means of a tracer particle[8] suitable dimensions of the draft-tube and its position in the vessel have been derived, so that the entire charge would be more uniformly affected by the energy-rich flow from the impeller.

The spacial distribution of streamlines in the region where the circulation has thus been improved could not be determined by following the circulation of the tracer particle, as the available numerical solution of the partial differential equation[5] for the streamlines distribution in the region in question required a more detailled and time-consuming experimental investigation of the velocity distribution at its boundaries. Therefore a way of description of the liquid flow in the part of the vessel above the rotating impeller (or above the upper base of the draft-tube) has been considered based on an analytical solution of the partial differential equation describing the distribution of streamlines in this part of the agitated charge.

THEORETICAL

The mixed system under consideration consists of a cylindrical vessel and of an axial high-speed impeller (a propeller or a paddle agitator with flat, inclined blades). In the vessel there are radial baffles near the wall or the system with a draft-tube. In the case of the draft-tube, an impeller is placed in the cylindrical part of the draft-tube. The sense of rotation of the impeller is always such that the liquid is forced to the bottom. The system is filled with Newtonian liquid to the extent that the stationary height H of the liquid level above a flat bottom or above the horizontal plane dividing cylindrical and conical sections of the vessel equals the inside diameter D of the vessel. The flow of the stirred liquid is turbulent. In this agitated system, a cylindrical coordinate system (Figs 1, 2) is defined. Its origin coincides with the point of intersection of the axis of symmetry of the cylindrical vessel (the coordinate axis z) and the flat bottom (or the horizontal plane dividing the cylindrical and the conical parts of the vessel). Within the volume of the charge, region V_{II} above the impeller (or above the upper base of the draft-tube) is defined, which is confined by the cross-section S_{II}, the liquid level, and the respective part of the wall with radial baffles or grips for fastening the draft-tube. For liquid flow in this region the following simplifying assumptions are introduced: (*A*.1) The agitated liquid is incompressible. (*A*.2) Region V_{II} is axisymmetrical. (*A*.3) The flow pattern relates to the stationary state. (*A*.4).

The exchange of mass between region V_{II} and its surroundings takes place only through the cross-section S_{II}. (A.5). The flow velocity on the surface equals practically zero. (A.6) The flow in region V_{II} is supposed to be irrotational.

Let us define dimensionless quantities by the following relations:

$$R \equiv r/D\,, \qquad Z \equiv z/H\,, \qquad (1a, 1b)$$

$$W_{ax} \equiv \bar{w}_{ax}/(\pi\, dn)\,, \quad W_{rad} \equiv \bar{w}_{rad}/(\pi\, dn)\,, \qquad (2a, 2b)$$

$$\Psi \equiv \psi/(nd^3)\,. \qquad (3)$$

The solution is based on the mathematical model described in Fig. 3. For the calculation, the point $r = 0$; $z = $ H is taken as origin of coordinates and reversed orientation of the z-axis is chosen according to the substitution

$$z' = H - z\,. \qquad (4)$$

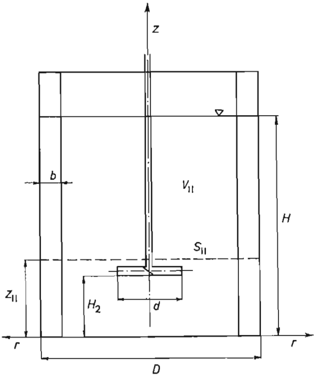

FIG. 1

Standard Agitated System with Axial High-Speed Impeller Placed in Axis and with Radial Baffles at Vessel Wall

Six blade impeller with inclined plane blades ($\alpha = 45°$). $H_2/D = 1/4$. 4 radial baffles $b/D = 1/10$, $d/D = 1/5$; $1/4$; $1/3$; $H/D = 1$; $D = 290$ mm.

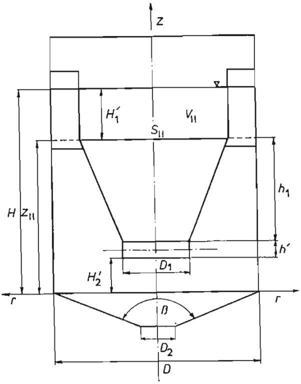

FIG. 2

Agitated System with High-Speed Impeller Placed in Axis and with Draft-Tube[8,9]

Six blade impeller with inclined plane blades ($\alpha = 45°$). $D_1/D = 0{\cdot}367$; $D_3/D = \sqrt{2}/2$; $H_2'/D = 1/10$; $h/D = 0{\cdot}067$; $h_1/D = 3/4$; $d/D = 1/3$; $H/D = 1$; $D = 290$ mm.

The distribution of streamlines in the investigated region may be described by the Stokes stream function $\psi(r, z')$ which is a solution of the partial differential equation[11]

$$\frac{\partial^2 \psi}{\partial z'^2} + \frac{\partial^2 \psi}{\partial r^2} - \frac{1}{r}\frac{\partial \psi}{\partial r} = 0\,, \tag{5}$$

satisfying the boundary conditions

$$\psi(0, z') = \psi(D/2; z') = 0\,, \quad [z' \in \langle 0; z'_{\mathrm{II}} \rangle] \tag{6a}$$

$$\psi(r, 0) = 0\,, \quad [r \in \langle 0; D/2 \rangle] \tag{6b}$$

$$-\bar{w}_{\mathrm{ax}}(r, z'_{\mathrm{II}}) = (1/r)\,\partial\psi(r, z'_{\mathrm{II}})/\partial r = f(r)\,. \quad [r \in \langle 0; D/2 \rangle] \tag{6c}$$

In the cross-section S_{II} between the regions V_{I} and V_{II}, the radial profile of the component $\bar{w}_{\mathrm{ax}}$, *i.e.* the shape of the function $f(r)$, is determined by a piston flow. In the boundary between the regions V_{II} and V_{III} the profile of this component is linear with maximum value at $r = D/2$ and minimum value (being the zero value of the component $\bar{w}_z$) at $r = \delta D/2$ (Fig. 4). Taking into account the equation of continuity for incompressible fluid, the boundary condition $f(r)$ at the cross-section S_{II} is finally defined as follows:

$$f(r) = \gamma\, f_0(r)\,, \tag{7}$$

and

$$f_0(r) = \begin{cases} 8nd(d/\delta D)^2\,, & [r \in \langle 0; \delta D/2 \rangle] \quad (8a) \\ -48nd(d/D)^2 \dfrac{r/D - \delta}{(1-\delta)^2\,(2+\delta)}\,. & [r \in \langle \delta D/2; D/2 \rangle] \quad (8b) \end{cases}$$

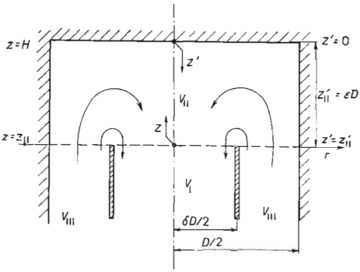

FIG. 3

Scheme of Mathematical Model of Flow in Region V_{II}

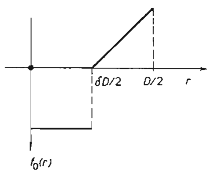

FIG. 4

Velocity Profiles on Boundaries of Regions V_{I} and V_{II} and V_{I} and V_{III}

The choice of $\gamma = 1$ corresponds to the nominal flow rate of 2π m^3 s^{-1} entering or leaving the volume V_{II} and to the unit value of the stream function on the interface of regions V_{I} and V_{III} in the cross-section S_{II}, *i.e.*

$$\psi(\delta D/2), z') = 1 \ \mathrm{m^3 \, s^{-1}} , \quad [z' \geqq z'_{\mathrm{II}}] . \tag{9}$$

Let us further have

$$z'_{\mathrm{II}} = \varepsilon D \tag{10}$$

and the mathematical model is then defined by the diameter D, the two dimensionless parameters δ, ε describing the geometry of the arrangement, and the dimensionless parameter γ determining the flow velocity with regard to the nominal flow $\psi(\delta D/2, \varepsilon D)$ defined by (*9*).

Separation of variables

$$\psi(r, z') = \varrho(r) \, . \, \xi(z') \tag{11}$$

leads to differential equations[12]

$$\frac{\mathrm{d}^2 \varrho}{\mathrm{d}r^2} - \frac{1}{r}\frac{\mathrm{d}\varrho}{\mathrm{d}r} + \lambda^2 \varrho = 0 , \tag{12}$$

$$\frac{\mathrm{d}^2 \xi}{\mathrm{d}z'^2} - \lambda^2 \xi = 0 \tag{13}$$

with boundary conditions

$$\xi(0) = 0 , \quad \varrho(0) = \varrho(D/2) = 0 . \tag{14a, 14b}$$

The convenient fundamental system of independent solutions for Eq. (*12*) is $r \, \mathrm{J}_1(\lambda r)$, $r \, \mathrm{Y}_1(\lambda r)$ and for Eq. (*13*) $\sinh \lambda z'$, $\cosh \lambda z'$.

Boundary conditions (*14*) require solutions in the following form: const $r \, \mathrm{J}_1(2\lambda_k \, . \, r/D) \, . \, \sinh(2\lambda_k z'/D)$, where λ_k are zeros[13] of the Bessel function of the first kind $\mathrm{J}_1(z')$. Thus the Stokes stream function is obtained in the following series representation:

$$\psi(r, z') = nd^3(2\gamma/D) \sum_{k=1}^{\infty} A_k r \, \mathrm{J}_1(2\lambda_k r/D) \sinh(2\lambda_k z'/D) . \tag{15}$$

Axial and radial components of the mean time velocity are

$$\bar{w}_{\mathrm{ax}} = -(1/r) \, \partial\psi/\partial r , \quad \bar{w}_{\mathrm{r}} = (1/r) \, \psi\partial/\partial z' , \tag{16a, 16b}$$

Hence

$$\bar{w}_{ax}(r, z') = -4nd\,\gamma(d/D)^2 \sum_{k=1}^{\infty} A_k\lambda_k\, J_0(2\lambda_k r/D) \sinh(2\lambda_k z'/D)\,, \qquad (17a)$$

$$\bar{w}_r(r, z') = 4nd\,\gamma(d/D)^2 \sum_{k=1}^{\infty} A_k\lambda_k\, J_1(2\lambda_k r/D) \cosh(2\lambda_k z'/D)\,. \qquad (17b)$$

Coefficients A_k are obtained from boundary condition (*6c*) for $z' = \varepsilon D$, that is to say

$$f(r) = 4nd\,\gamma(d/D)^2 \sum_{k=1}^{\infty} A_k\lambda_k\, J_0(2\lambda_k r/D) \sinh(\varepsilon\lambda_k)\,,$$

in the usual way[13]:

$$4nd\,\gamma(d/D)^2\, A_k\lambda_k \sinh(\varepsilon\lambda_k) = \|J_0(2\lambda_k r/D)\|^{-2} \int_0^{D/2} r\, f(r)\, J_0(2\lambda_k r/D)\, dr\,,$$

where

$$\|J_0(2\lambda_k r/D)\|^{-2} = 8/[D^2\, J_0^2(\lambda_k)]\,.$$

Finally, with respect to Eqs (*7*) and (*8*) we have

$$A_k = 4[\delta\lambda_k^2\, J_0(\lambda_k) \sinh(\varepsilon\lambda_k)]^{-1} \,.\, [J_1(\delta\lambda_k) + 3\delta\{\delta\, J_0(\delta\lambda_k) - $$
$$-J_0(\lambda_k) - \lambda_k^{-1}[m(\delta\lambda_k) - m(\lambda_k)]\} \,.\, [\lambda_k(1-\delta)^2\,(2+\delta)]^{-1}]\,, \qquad (18)$$

where

$$m(x) = \int_0^x J_0(y)\, dy\,. \qquad (19)$$

For the agitated system under consideration H equals D and the dimensionless variables W_{ax}, W_{rad} and Ψ (Eqs (*2*) and (*3*)) and dimensionless arguments R and Z (Eq. (*1*)) are defined. If the transformation

$$z'/D = (1 - Z) \qquad (20)$$

is applied, we have the following results valid in region V_{II}:

$$\Psi(R, Z) = (2\gamma/nd^3) \sum_{k=1}^{\infty} A_k R\, J_1(2\lambda_k R) \sinh[2\lambda_k(1 - Z)]\,, \qquad (21a)$$

$$W_{ax}(R, Z) = -(4\gamma/\pi)\,(d/D)^2 \sum_{k=1}^{\infty} A_k\lambda_k\, J_0(2\lambda_k R) \sinh[2\lambda_k(1 - Z)]\,, \qquad (21b)$$

$$W_{rad}(R, Z) = (4\gamma/\pi)(d/D)^2 \sum_{k=1}^{\infty} A_k \lambda_k \, J_1(2\lambda_k R) \cosh(2\lambda_k(1 - Z)] \,. \qquad (21c)$$

With $R \in \langle 0; 1/2 \rangle$ and $Z \in \langle Z_{II}; 1 \rangle$, where $Z_{II} = z_{II}/H$, that is at any point of the investigated region V_{II}, the sought kinematic characteristics may be calculated from Eqs (*21*).

EXPERIMENTAL

Flow Measurements

The liquid flow in both types of agitated systems was investigated either by measurements of pressure using directional Pitot tubes[4] (in the standard system with radial baffles — Fig. 1) or by the measurement of circulation time of a tracer particle[8,9] (the system with a draft-tube). The liquid used was water or water solutions of glycerol. The conditions in the system were always such that the type of flow within it was turbulent, *i.e.* the value of the mixing Reynolds number $Re_M > 1{\cdot}0 \,.\, 10^4$. In all experiments, the frequency of revolution of impeller n, the kinematic viscosity of liquid ν and the impeller diameter d, were considered as independent variables. In case of the local measurements of pressure in the charge, the total pressures taken from the individual holes of the directional Pitot tube were chosen as dependent variables. In case of the measurements using the tracer particle, the circulation time τ was taken as dependent variable, *i.e.* the time interval during which the particle (representing by its shape and behaviour a particle of the flowing liquid[14]) would complete a circulation loop between two subsequent crossings of the upper base of the draft-tube. For agitating the charge a standard six blade paddle impeller with flat, inclined blades ($\alpha = 45°$) was used[15]. The impeller was placed in the axis of the cylindrical vessel and its direction of rotation was that to force the liquid to the bottom.

Calculation of Streamlines Pattern

The calculation of the pattern of streamlines in region V_{II} was carried out on the TESLA 200 computer using equations (*21*), from which, together with the dimensionless Stokes stream function $\Psi(R, Z)$, the values of $W_{ax}(R, Z)$ and $W_{rad}(R, Z)$ were obtained as functions of position in the considered region. The subroutine for the computations of the Bessel functions $J_0(x)$, $J_1(x)$ and of $m(x)$ in Eq. (*19*) was for small $x (x < 20)$ based on the sum of a power series representation, and for large x ($x \in \langle 20; 50 \rangle$) on an asymptotic expansion[13]. Roots λ_k of the Bessel function $J_1(x)$ were transferred from tables[16] and the whole calculation was performed with double precision — *i.e.* with 14 non-zero digits. The quantities δ and ε characterizing the geometry of region V_{II} were obtained from the arrangements of the two investigated types of systems. The following values have been used:

For the standard system: $\delta = \sqrt{2}/2$; $d/D = 1/5$; $1/4$, $1/3$;

$\gamma = 0{\cdot}514, 0{\cdot}382, 0{\cdot}314$; $\varepsilon = 0{\cdot}69$.

For the system with a draft-tube: $\delta = \sqrt{2}/2$; $d/D = 1/3$;

$\gamma = 0{\cdot}113$; $\varepsilon = 2^{1/2}/8$.

The coefficient γ expresses, in a dimensionless form, the maximum value of stream function in the cross-section S_{II}. It was determined from the known discharge rate in the respective cross-section and in the given direction (upwards or downwards), according to the relation

$$\gamma = \Psi[\delta D/2, (1 - \varepsilon) D] = Kc_{II}/2\pi \equiv (1/2\pi)(\dot{V}v_{II}/nd^3). \qquad (22)$$

The overall flow rate $\dot{V}_{CII}$ in the cross-section S_{II} in the given direction was for the standard arrangement with radial baffles evaluated from the profile of the velocity component $\overline{w}_{ax}[r, (1 - \varepsilon) D]$. The latter was determined from the pressure distribution measured in this cross-section by means of directional Pitot tubes[4,17]. For the system with the draft-tube $\dot{V}_{CII}$ was determined from the mean circulation time $\bar{\tau}$ of the tracer particle, using relations[8,9]

$$\dot{V}_{CII} = V/\bar{\tau}, \qquad (23)$$

where V is total volume of the charge. Moreover, as there had been set up several levels of quantities n and v, for the considered geometric arrangement of the system, the mean value of the overall flow rate criterion K_{CII} in the cross-section S_{II} (see relation (22)) was always obtained as the arithmetic mean of values at the respective levels of variables. At the same time, the fact that K_{CII} does not depend on Re_M, as far as $Re_M > 1{\cdot}0 \,.\, 10^4$, was taken into account.

RESULTS AND DISCUSSION

Streamlines Pattern in a System with Axial High-Speed Agitator

Figs 5–7 show the patterns of streamlines in the volume V_{II} above the rotating high-speed impeller in the baffled vessel. In Fig. 8 the flow pattern in the vessel

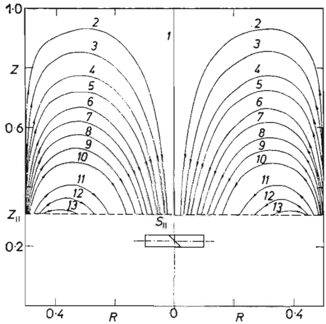

FIG. 5

Streamlines Pattern in Section V_{II} (standard cylindrical system with axial high-speed impeller and radial baffles, $d/D = 1/5$)

1 0; *2* 0·002; *3* 0·005; *4* 0·01; *5* 0·015; *6* 0·025; *7* 0·035; *8* 0·05; *9* 0·07; *10* 0·1; *11* 0·2; *12* 0·3; *13* 0·45.

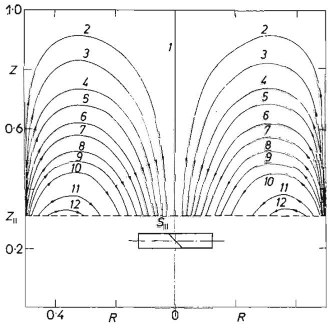

FIG. 6

Streamlines Pattern in Section V_{II} (standard cylindrical system with axial high-speed impeller and radial baffles, $d/D = 1/4$)

1 0; *2* 0·002; *3* 0·005; *4* 0·01; *5* 0·015; *6* 0·025; *7* 0·035; *8* 0·05; *9* 0·07; *10* 0·1; *11* 0·2; *12* 0·3.

with a draft-tube is shown. These spacial distributions have been obtained by solving equation (5) under consideration of a definite distribution of the flow function on the boundary of the region investigated (see system of equations (6) to (8)). The solution of the boundary-value problem in Eqs (5)–(6) and (12)–(13) is $\Psi(R, Z)$ as given in Eq. (21a) and graphically expressed in Figs 5–8. The curves with constant values of the dimensionless Stokes function Ψ = const describe the flow pattern, as the stream function is constant along a streamline. The value of this constant is marked against each streamline in Figs 5–8. The dashed line represents the projection of the boundary of region V_{II}, namely the cross-section S_{II}.

In Fig. 9 are drawn the velocity profiles $W_{ax} = W_{ax}(R, Z_{II})$ for the cases solved, *i.e.* the profiles of the dimensionless axial component of the mean velocity in the cross section S_{II} (with the coordinate Z_{II}). Here, the solid lines represent the velocity component profiles on the boundary of the investigated section obtained from relation (21b). The dashed lines represent the given profiles, *i.e.* the functions $f(r)$ or $f_0(r)$ from Eqs (7) and (8), here expressed in dimensionless form:

$$F(R) = \gamma F_0(R), \qquad (24)$$

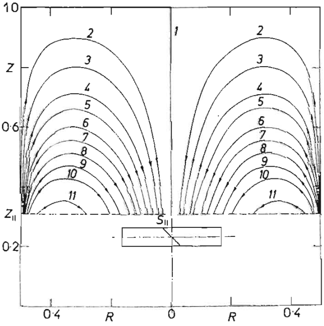

FIG. 7

Streamlines Pattern in Section V_{II} (standard cylindrical system with axial high-speed impeller and radial baffles, $d/D = 1/3$)

1 0; *2* 0·002; *3* 0·005; *4* 0·01; *5* 0·015; *6* 0·025; *7* 0·035; *8* 0·05; *9* 0·07; *10* 0·1; *11* 0·2.

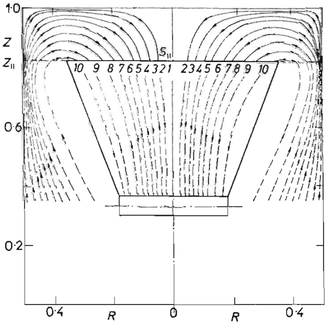

FIG. 8

Streamlines Pattern in Section V_{II} (cylindrical system with axial high-speed impeller and draft-tube, $d/D = 1/3$)

1 0; *2* 0·002; *3* 0·005; *4* 0·01; *5* 0·015; *6* 0·25; *7* 0·035; *8* 0·05; *9* 0·07; *10* 0·1. ——— calculated streamlines, ----- supposed course of streamlines.

$$F_0(R) = \begin{cases} -(8/\pi)(d/\delta D)^2, & [R \in \langle 0; \delta/2 \rangle], \quad (25a) \\ 48(d/D)^2 \dfrac{R - \delta}{\pi(1 - \delta)^2 (2 + \delta)}, & [R \in \langle \delta/2; 1/2 \rangle]. \quad (25b) \end{cases}$$

(In relations (*24*) and (*25*) the direction of the z-axis coincides with that in Figs 1 and 2; it differs from the direction in Figs 3 and 4 and in equations (*7*) and (*8*) where the opposite orientation was introduced only for the sake of convenience.)

Discussion of Validity of Simplifying Assumptions

Out of the six assumptions introduced, assumption (*A.1*) on the liquid incompressibility, as well as (*A.3*), on the stationarity (or better, quasistationarity) of flow, are evidently satisfied for current types of stirred charges (*e.g.* liquids or liquid–liquid and liquid–solid dispersions). As a rule, these systems are stirred for a sufficiently long time in comparison with the interval after which, frequency of revolu-

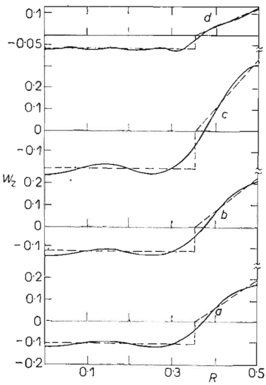

FIG. 9

Comparison of Experimentally Obtained and Calculated Velocity Profiles $W_{ax} = W_{ax}(R)$ . . $[Z = Z_{II}]$ in Cross-section S_{II}

– – – – – Velocity profile obtained experimentally, ——— velocity profile calculated; *a* $d/D = 1/5$; *b* $d/D = 1/4$; *c* $d/D = 1/3$; *d* draft-tube.

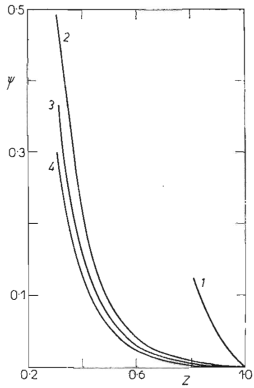

FIG. 10

Graph of Function $\Psi = \Psi(Z)$ for $R = \delta/2$

Profile *4*: Arrangement: standard system $d/D = 1/5$; Profile *3*: Arrangement: standard system $d/D = 1/4$; Profile *2*: Arrangement: standard system $d/D = 1/3$; Profile *1*: Arrangement: draft-tube $d/D = 1/3$.

tion being constant, no further changes of the circulation take place. The axial symmetry of the region V_{II} (*A.2*) is apparently not complete. However, the influence of radial baffles or draft-tube grips manifests itself in a very small part of this section, so that it may be neglected. In the considered case, the agitated system has no flow-through. Hence the stirred medium enters and leaves V_{II} only through S_{II} (*A.4*). As the vessel is fitted with baffles and the flow is directed downwards, the liquid surface may be considered calm (*A.5*). Assumption (*A.6*) on the irrotational flow in the region V_{II} (above the impeller) may appear rather daring, but it is supported by the results of our experimental investigation of the velocity field in the agitated system: In the examined region, the volumetric rate of mechanical energy dissipation is very low, in comparison with other parts of the system. Only 10% of the total agitator power input is dissipated here (in case of the standard system, Fig. 1). Also the mean velocity profiles at the entrance of the section (Fig. 9) and within it (Fig. 11) are very flat, which implies low values of velocity gradients and low shear stresses. Thus the proposed description of the velocity distribution by means of the equation of irrotational flow appears as adequate and feasible for analytical solution leading to an integral description of convection flow in V_{II}, though, for an exact description, the Reynolds equations of time averaged flow of incompressible fluid[11] should be used.

In examining the adequacy of the introduced assumptions the degree of correspondence of the suggested solution to the actual flow pattern in the region ought to be also assessed. In the first place, the suggested velocity profile $W_{ax} = W_{ax}(R, Z_{II})$

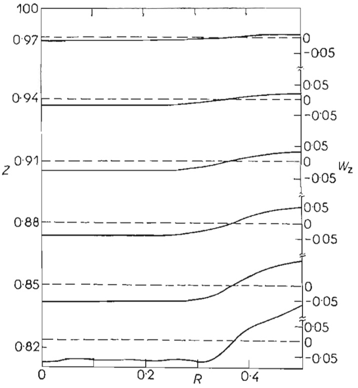

FIG. 11

Dependence of Velocity Profile $W_{ax} = W_{ax}(R)$ on Value of Dimensionless Axial Coordinate Z (agitated system with draft-tube; $d/D = 1/3$)

is to be compared with the corresponding experimental results, the shape of the profile has indeed been confirmed in an experimental way to conform[4] with equations (24)–(25) and (7)–(9). It is, however, necessary to mention the fact that in the surroundings of the point $R = \delta/2$, the direction of the velocity vector changes not stepwise, but continuously. This also implies that the calculated velocity profile is nearer to the real one than the given function $F(R)$ itself, considered as the boundary condition of the solution of equations (5) in V_{II}, although the difference between the prescribed and the calculated profiles (Fig. 9) is here the greatest, due to the adopted accuracy of calculation of the Bessel functions. The distribution of streamlines in the whole volume above the rotating impeller does not differ from the real one in more than $\pm 10\%$, which is in accord with the accuracy of local velocity measurements in the examined sections[18]. This error, however, significantly increases in the vicinity of the vessel wall, as the irrotational flow solution cannot correctly describe the conditions in the boundary layer. A corollary of this is the fact that the proposed description of the convection flow in V_{II} relates to the flow in the bulk of liquid and to the processes controlled by it (*e.g.* blending of miscible liquids, suspension of particulate solids *etc.*). To this end the solution was sought in the form of a system of equations interpreting the convective flow intensity, which would be suitable for description of such processes.

Homogenation of Streamlines Field

Both the issues of experimental investigation of spacial distribution of mechanical energy dissipation in the system with an axial impeller and radial baffles[4], and the results of the calculations of spacial distribution of the liquid circulation intensity carried out in this contribution, show that above the impeller, even in the case of turbulent regime, mixing is brought about mainly by the convection flow of the agitated medium. Moreover, nearly a third of the liquid volume included in this space (*i.e.* a part of the volume V_{II}, whose dimensionless axial coordinate Z_{II} is from the interval $\langle 0{\cdot}65; 1\rangle$) is flown through by almost the same quantity of liquid, disregarding the relative size of the impeller d/D (Fig. 10). The spacial distribution of streamlines in this subsection is also practically independent of the impeller-to-vessel diameter ratio. Therefore it may be concluded that the suggested construction of the draft-tube[9] corresponding in shape to that proposed for the improvement of blending of miscible liquids[19], will have a favourable influence on the spacial distribution of circulation as it has been in the systems evaluated in this study. Here, the volumetric flow rate through the cross-section with the dimensionless coordinate $Z = 1 - \sqrt{2}/8$ in one direction (upwards or downwards), increased, after installing the draft-tube, to more than one order with respect to the standard conditions (Fig. 10), the flow intensity above this cross-section having increased similarly (Figs 8 and 9). This fact has been reflected also by the profiles of the axial component of mean velocity in this arrangement (Fig. 11) being significantly non-zero, even near the liquid surface. Worth mentioning is also the invariability of the position of the boundary between the ascending and decsending flows (dimensionless radial coordinate $R = \delta/2$) with increasing Z: this is an evidence of appropriate choice of the upper base diameter of the draft-tube D_3, so that equal upflow and downflow areas might be obtained. (This corresponds to the value $Z = 1 - \varepsilon = 1 - \sqrt{2}/8$ introduced earlier.) Therefore, the type of the draft-tube proposed here may be useful especially in such operations where a high degree of homogeneity of velocity distribution is desirable, *e.g.* in agitated crystallizers, homogeneous mixed reactors *etc.*, where the whole volume filled with the charge should contribute to producing the output of a technological process.

The authors are obliged to express their thanks to Mrs M. Špicarová for her invaluable help in preparing figures included in this paper.

LIST OF SYMBOLS

A_k	coefficient in Eq. (*15*)
b	width of radial baffle, m
d	diameter of impeller, m
D	diameter of vessel, m
D_1	diameter of lower (cylindrical) part of draft-tube, m
D_3	diameter of upper base of draft-tube, m
D_2	diameter of outlet of crystals from model crystallizer, m
$f(r)$	function defined by Eq. (*7*)
$f_0(r)$	function defined by Eq. (*8*)
$F(R)$	function defined by Eq. (*24*)
$F_0(R)$	function defined by Eq. (*25*)
h	height of impeller blade, m
h'	height of cylindrical part of draft-tube, m
h_1	height of conical part of draft-tube, m
H	height of still liquid level above flat bottom of vessel or above horizontal plane dividing cylindrical and conical sections of vessel, m
H_2	height of lower edge of blades above flat bottom of vessel, m
H_2'	height of lower edge of blades above horizontal plane dividing cylindrical and conical parts of vessel, m
J_0	Bessel function of the first kind of order 1
J_1	Bessel function of the first kind of order 2
K_{CII}	overall flow rate criterion in cross section S_{II}
$m(x)$	function defined by Eq. (*19*)
n	impeller frequency of revolution, s^{-1}
r	radial coordinate (radius), m
R	dimensionless radial coordinate
S_{II}	cross-section separating region V_{II} from the rest of agitated charge, m^2
V	total charge volume, m^3
V_{II}	charge volume above rotating impeller, m^3
V_I	region of inflow into volume V_{II}, m^3

V_{III} region of outflow from volume V_{II}, m^3
$\bar{w}$ mean time velocity, $m\,s^{-1}$
W dimensionless mean time velocity
x general variable
y general variable
Y_1 Bessel function of the second kind of order 1
z axial coordinate, m
z' transformed axial coordinate, m
Z dimensionless axial coordinate
α angle of inclination of impeller blades (from horizontal plane)
β angle of inclination of conical bottom of model crystallizer
γ value of dimensionless stream function at $r = \delta D/2$, $z = (1 - \varepsilon) D$
$\delta/2$ dimensionless radial coordinate of the point where the direction of flow changes in cross-section S_{II}
$1 - \varepsilon$ dimensionless axial coordinate of area S_{II}
λ_k Zeros of Bessel function $J_1(x)$
ψ Stokes stream function, $m^3\,s^{-1}$
Ψ dimensionless Stokes stream function
ν kinematic viscosity of liquid, $m^2\,s^{-1}$
ϱ variable in differential Eq. (*12*)
ξ variable in differential Eq. (*13*)
τ time of circulation of tracer particle, s
$Re_M = nd^2/\nu$ Reynolds number for mixing

Subscripts and Superscripts

ax axial
M for mixing
rad radial
II related to cross-section S_{II}
— time average quantity

REFERENCES

1. Rushton J. H., Oldshue J. Y.: Chem. Eng. Progr. *49*, 161, 267 (1953).
2. Porcelli J. V., Marr G. R.: Ind. Eng. Chem., Fundam. *1*, 172 (1962).
3. Fořt I., Valešová H., Kudrna V.: This Journal *36*, 164 (1971).
4. Fořt I., Neugebauer R., Pastyříková H.: This Journal *36*, 1769 (1971).
5. Fořt I., Gračková Z., Koza V.: This Journal *37*, 2371 (1972).
6. Fořt I., Koza V., Gračková Z.: This Journal *38*, 3074 (1973).
7. Fořt I., Hrubý M., Mošna P.: This Journal *38*, 1757 (1973).
8. Fořt I., Kudrna V., Vlček J.: Chem. Prům. *24*, 485 (1974).
9. Fořt I., Vlček J., Kudrna V.: Chem. Prům. *25*, 449 (1975).
10. Musil L.: This Journal *41*, 839 (1976).
11. Kotchin N. E., Kibel I. A., Roze N. V.: *Teoreticheskaya Gidromekhanika*. Gos. Izd. Fiz.-Mat. Lit., Moscow 1963.
12. Korn G. A., Korn T. M.: *Mathematical Handbook for Scienctists and Engineers*. McGraw-Hill, New York, London 1961.

13. Watson G. N.: *A Treatise on the Theory of Bessel Functions.* Cambridge University Press, Cambridge 1922.
14. Steidl H.: This Journal *23*, 1664 (1958).
15. Czechoslovak Standard 69 10 21.
16. Fadeeva V. N., Gavurin M. K.: *Tables of Bessel Functions* $J_n(x)$, (in Russian). Gos. Izd. Techn. Teor. Lit., Moscow, Leningrad 1950.
17. Fořt I., Podivínská J., Baloun R.: This Journal *34*, 959 (1969).
18. Pastyříková H., Fořt I.: Sb. Vys. Šk. Chemicko-Technol. Praze *K 4*, 41 (1971).
19. Landau J., Procházka J., Václavek V., Fořt I.: This Journal *36*, 1546 (1971).

Translated by M. Procházka.